

Related content

- [Extraction of an entanglement by repetition of the resonant transmission of an ancilla qubit](#)
Kazuya Yuasa
- [Resonant scattering can enhance the degree of entanglement](#)
Kazuya Yuasa and Hiromichi Nakazato
- [Entanglement-assisted tomography of a quantum target](#)
A De Pasquale, P Facchi, V Giovannetti et al.

To cite this article: Kazuya Yuasa *et al* 2009 *New J. Phys.* **11** 123027

View the [article online](#) for updates and enhancements.

Recent citations

- [Sensitivity of measurement-based purification processes to inner interactions](#)
Benedetto Militello and Anna Napoli
- [Manipulating quantum information with spin torque](#)
Brian Sutton and Supriyo Datta
- [Entanglement purification and amplification of three-qubit states using two-outcome weak measurements](#)
Xiang-Ping Liao *et al*

Efficient generation of a maximally entangled state by repeated on- and off-resonant scattering of ancilla qubits

Kazuya Yuasa^{1,5}, Daniel Burgarth², Vittorio Giovannetti³ and Hiromichi Nakazato⁴

¹ Waseda Institute for Advanced Study, Waseda University, Tokyo 169-8050, Japan

² IMS and QOLS, Imperial College, London SW7 2BK, UK

³ NEST-CNR-INFM & Scuola Normale Superiore, piazza dei Cavalieri 7, I-56126 Pisa, Italy

⁴ Department of Physics, Waseda University, Tokyo 169-8555, Japan

E-mail: yuasa@aoni.waseda.jp

New Journal of Physics **11** (2009) 123027 (19pp)

Received 18 September 2009

Published 21 December 2009

Online at <http://www.njp.org/>

doi:10.1088/1367-2630/11/12/123027

Abstract. A scheme for preparing two fixed noninteracting qubits in a maximally entangled state is presented. By repeating on- and off-resonant scattering of ancilla qubits, the target qubits are driven from an arbitrary initial state into a singlet state with probability 1 (perfect efficiency). Neither the preparation nor the post-selection of the ancilla spin state is required. The convergence from an arbitrary input state to the unique fixed point (mixing property) is proved rigorously, and its robustness is investigated by scrutinizing the effects of imperfections in the incident wave of the ancilla—such as mistuning to a resonant momentum, imperfect monochromatization, and fluctuation of the incident momentum—as well as detector efficiency.

⁵ Author to whom any correspondence should be addressed.

Contents

1. Introduction	2
2. Setup	3
3. Protocol	6
4. Proof	7
5. Robustness	10
5.1. Errors in the incident momentum	10
5.2. Detector efficiency	15
6. Conclusions and remarks	18
Acknowledgments	18
References	19

1. Introduction

How does one prepare a quantum state? This is an important problem that has to be tackled. In fact, various interesting and peculiar phenomena are predicted on the basis of highly nonclassical states, and entanglement plays a key role in quantum information protocols [1]. They all rely on the generation of nontrivial states and are not realized without establishing strategies for the preparation of such quantum states.

Generally speaking, we try to drive a quantum system to a specific state by a series of operations, e.g. applications of external fields to transform its state, measurements to project it onto a particular configuration and so on. A generic mechanism was found to extract a pure quantum state from a given arbitrary (mixed, in general) state, by simply repeating the same measurement on an ancilla system interacting with the target system [2, 3]. Such a mechanism is interesting in itself and is even indispensable when direct operations on target quantum systems are not allowed or unavailable. Repeated measurements on the ancilla can be regarded as an indirect (positive operator valued measure (POVM)) measurement on the target system, which, under proper conditions, allows us to drive the latter toward the desired pure state. This idea was applied to the initialization of qubits [3], to the extraction of entanglement [3, 4] and a nonclassical state [5], and to establish entanglement between separated qubits [6]–[9].

In those schemes, a pure quantum state is obtained from an arbitrary initial configuration only when the ancilla system is repeatedly confirmed to be in a specific state by all the measurements performed during the protocol. That is, they are probabilistic schemes characterized by a success probability strictly less than 1. The primary motivation of the present work is to pursue a scheme that would allow one to reach the target state with probability 1, or at least with probability arbitrarily close to 1, independently of the initial conditions. We have been inspired to achieve this by an approach recently introduced in [10], in which a target system is indirectly controlled by making it interact with a sequence of (properly prepared) ancillas, which are then discarded. As in the case of [10], our finding relies on a useful property of quantum channels. Namely, we make use of the fact that under proper conditions (see, for instance, [11, 12] and references therein) repetitive applications of the same map drive the system toward a fixed point, independently of its initial configuration (*mixing* property).

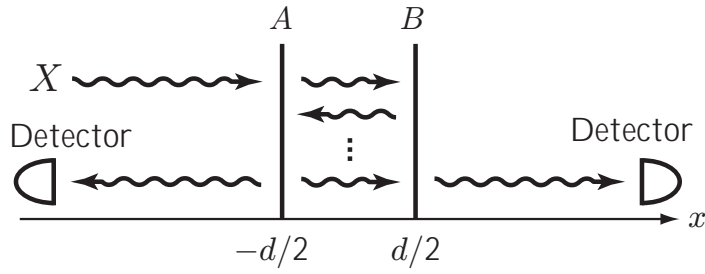


Figure 1. Schematic drawing of the setup. An ancilla qubit X is sent to two fixed qubits A and B , with a certain wave vector k . After being scattered by the delta-shaped potentials produced by A and B , we check whether it is reflected or transmitted. Neither the preparation of the spin of the incident X nor the spin-resolved detection of the scattered X is required.

As a nontrivial example of such a scheme, we concentrate on a prototypical setup that has been extensively investigated in the literature recently [7]–[9], [13]–[15]. Here, two noninteracting target qubits A and B sit at a fixed distance from each other along a one-dimensional (1D) channel, as sketched in figure 1. The goal of the scheme is to drive A and B into an entangled state with the help of a (flying) qubit, which is sent through the 1D channel and is detected after it has been scattered by the targets. In the simplest configuration considered so far, the latter are supposed to be initially in a (known) separable state, while the ancilla qubit is prepared in an appropriate spin state before being injected into the setup. Under these assumptions, it has been shown that entanglement between A and B can be generated in a probabilistic fashion by a simple post-selection of the spin state of the scattered ancilla [13]–[15]. Schemes that do not require preparation of the initial state of the target qubits to a specific state were also proposed, in which entanglement is extracted after repetition of scattering + post-selection [7]–[9]. Improved protocols such as these, however, are still probabilistic, as they produce the desired entanglement only with a certain probability of success. By contrast, the approach we present here generates a maximally entangled state between A and B from an arbitrary initial state with probability 1. Furthermore, it requires neither the preparation nor the post-selection of the spin state of the ancilla qubits.

The present paper is organized as follows. In section 2, we introduce the setup and present some preliminary definitions. Section 3 introduces the protocol and states the main result of our work. The proof of the latter is then provided in section 4. Section 5 analyzes the robustness of the scheme, whereas conclusions and remarks are given in section 6.

2. Setup

Our setup is sketched in figure 1. Two qubits A and B are fixed at $x = -d/2$ and $d/2$, respectively, along a 1D channel. They do not interact directly, although we wish to establish entanglement between them. To do so, we send flying ancilla qubits X as ‘mediators’ and let them scatter with A and B . As in [7]–[9, 13, 14], we assume the system to be described by the following Hamiltonian

$$H = \frac{p^2}{2m} + g(\boldsymbol{\sigma}^{(X)} \cdot \boldsymbol{\sigma}^{(A)})\delta(x + d/2) + g(\boldsymbol{\sigma}^{(X)} \cdot \boldsymbol{\sigma}^{(B)})\delta(x - d/2), \quad (2.1)$$

where x and p are the position and the momentum of X in 1D, the operators $\sigma^{(J)}$ ($J = X, A, B$) represent the Pauli operators of the spins, and the potentials produced by A and B are represented by the delta-shaped potentials. According to equation (2.1), the spin of X interacts separately with A and B through Heisenberg-type coupling during the scattering. This Hamiltonian has been proposed to effectively model the coupling between electrons occupying the lowest subband and magnetic impurities placed along a quasi-1D wire, such as a semiconductor quantum wire [16] or a single-wall carbon nanotube [17], where electrons flow.

Particle X is sent from the left with a fixed incident wave vector $k > 0$ and scattered by A and B . Matrix elements of the scattering operator S are given by [8, 15]

$$\langle k' \zeta' | S | k \zeta \rangle = e^{-ikd} [\delta(k' - k) \langle \zeta' | T_k | \zeta \rangle + \delta(k' + k) \langle \zeta' | R_k | \zeta \rangle], \quad (2.2)$$

where $|k\rangle$ is the eigenstate of the momentum operator p of X belonging to its eigenvalue $\hbar k$, and $|\zeta\rangle$ represents a spin state of XAB . Operators T_k and R_k describe the changes provoked in the spin state of XAB when X is transmitted to the right and reflected to the left, respectively. They satisfy the unitarity condition

$$T_k^\dagger T_k + R_k^\dagger R_k = \mathbb{1}_{XAB}, \quad (2.3)$$

and are given by

$$T_k = e^{ikd} [\alpha_k (1 - 4i\Omega_k) P_- + (\alpha_k Q_{1/2} + \beta_k Q_{3/2}) P_+ - \alpha_k \Omega_k^2 (1 - e^{2ikd}) (P_- - 3Q_{1/2} P_+ - K_+ + K_-)], \quad (2.4a)$$

$$R_k = T_k e^{-ikd} - 1 - i\Omega_k (1 - e^{2ikd}) \left\{ 6\alpha_k \Omega_k^2 (1 - e^{2ikd}) P_- + (2\alpha_k Q_{1/2} - \beta_k Q_{3/2}) P_+ + \frac{1}{2} \alpha_k [1 + 3\Omega_k^2 (1 - e^{2ikd}) - 4i\Omega_k P_+] (K_+ + K_-) \right\}, \quad (2.4b)$$

where

$$\alpha_k = \frac{1}{(1 - 4i\Omega_k) + 2\Omega_k^2 (1 - 6i\Omega_k) (1 - e^{2ikd}) + 9\Omega_k^4 (1 - e^{2ikd})^2}, \quad (2.5a)$$

$$\beta_k = \frac{1}{(1 + 2i\Omega_k) - \Omega_k^2 (1 - e^{2ikd})}, \quad \Omega_k = \frac{mg}{\hbar^2 k}. \quad (2.5b)$$

In the above expressions,

$$P_- = \frac{1 - \sigma^{(A)} \cdot \sigma^{(B)}}{4}, \quad P_+ = \frac{3 + \sigma^{(A)} \cdot \sigma^{(B)}}{4} \quad (2.6)$$

are the projection operators on the singlet and triplet sectors of A and B , respectively, whereas

$$Q_{3/2} = \frac{2}{3} P_+ + \frac{1}{6} \sigma^{(X)} \cdot (\sigma^{(A)} + \sigma^{(B)}), \quad (2.7a)$$

$$Q_{1/2} = P_- + \frac{1}{3} P_+ - \frac{1}{6} \sigma^{(X)} \cdot (\sigma^{(A)} + \sigma^{(B)}) \quad (2.7b)$$

are those on the spin- $\frac{3}{2}$ and spin- $\frac{1}{2}$ sectors of XAB , respectively [15] (note that they are all commuting with each other and satisfy $Q_{3/2} P_- = P_- Q_{3/2} = 0$).⁶ The other operators

$$K_\pm = \sigma^{(X)} \cdot \Sigma_\pm^{(AB)}, \quad (2.8)$$

⁶ Throughout this paper, unit operators are often omitted as $\mathbb{1}_X \otimes P_\pm \rightarrow P_\pm$, $\mathbb{1}_X \otimes \sigma^{(A)} \otimes \mathbb{1}_B \rightarrow \sigma^{(A)}$, $3\mathbb{1}_{AB} \rightarrow 3$, etc.

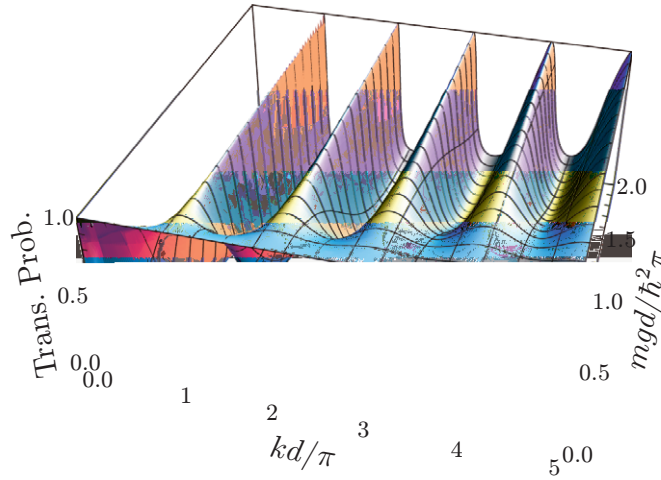


Figure 2. Transmission probability of the ancilla qubit X when it is injected from the left with its spin prepared in $|\uparrow\rangle_X$. The plot shows the probability of detecting the ancilla on the right detector after the scattering by A and B . Here, A and B are assumed to be initially in the singlet state $|\Psi^-\rangle_{AB}$, so that the quantity plotted is nothing but $\text{Tr}\{T_k(|\uparrow\rangle_X\langle\uparrow| \otimes |\Psi^-\rangle_{AB}\langle\Psi^-|)T_k^\dagger\}$. Its dependence on the incident wave vector k of X and the coupling constant g is shown. It exhibits resonances at $k = n\pi/d$ ($n = 1, 2, \dots$) for any $g \neq 0$.

defined with

$$\begin{aligned}
 \Sigma_+^{(AB)} &= \frac{1}{2}[(\sigma^{(A)} - \sigma^{(B)}) + i(\sigma^{(A)} \times \sigma^{(B)})] \\
 &= P_+(\sigma^{(A)} - \sigma^{(B)}) = P_+i(\sigma^A \times \sigma^B) \\
 &= (\sigma^{(A)} - \sigma^{(B)})P_- = i(\sigma^A \times \sigma^B)P_- \\
 &= \Sigma_-^{(AB)\dagger},
 \end{aligned} \tag{2.9}$$

are responsible for transitions between the singlet and triplet sectors of A and B , with the only nonzero elements $P_\pm \Sigma_\pm^{(AB)} P_\mp \neq 0$.

It is pointed out in [14] that this system exhibits interesting resonant transmissions controlled by the entanglement in A and B ; for instance, when A and B are in the singlet state $|\Psi^-\rangle_{AB} = (|\uparrow\downarrow\rangle_{AB} - |\downarrow\uparrow\rangle_{AB})/\sqrt{2}$, the potentials produced by A and B look ‘transparent’ for X sent with a resonant wave vector k_n satisfying the resonance condition $k_n d = n\pi$ ($n = 1, 2, \dots$) (see figure 2). More explicitly, the transmission and reflection operators T_k and R_k at the resonance points are given by

$$T_{k_n} = (-1)^n \left[P_- + \left(\frac{Q_{1/2}}{1 - 4i\Omega_{k_n}} + \frac{Q_{3/2}}{1 + 2i\Omega_{k_n}} \right) P_+ \right], \tag{2.10a}$$

$$R_{k_n} = \left(\frac{4i\Omega_{k_n}}{1 - 4i\Omega_{k_n}} Q_{1/2} - \frac{2i\Omega_{k_n}}{1 + 2i\Omega_{k_n}} Q_{3/2} \right) P_+, \tag{2.10b}$$

showing that X is perfectly transmitted without spin flip when A and B are in the singlet state $|\Psi^-\rangle_{AB}$.

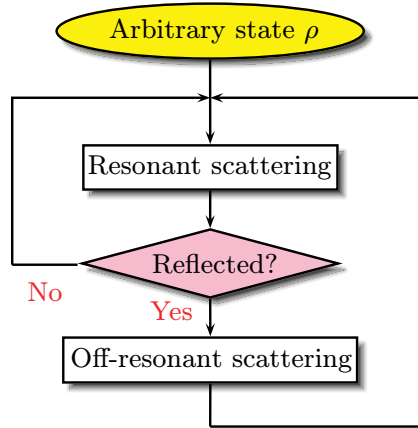


Figure 3. Flowchart of the protocol.

3. Protocol

To construct our scheme, we make use of the resonance condition detailed in the previous section. Similar approaches have been explored in [7]–[9]. Specifically, in [7] Ciccarello *et al* exploited repetition of the scattering of X with a resonant momentum followed by an appropriate post-selection on X to extract the singlet state $|\Psi^-\rangle_{AB}$ from AB with a probability dependent on the initial state of the system. By contrast, in [8, 9] a scheme to extract the singlet state from an arbitrarily given initial state of AB is proposed, in which neither the preparation of the spin state of X nor its post-selection is required. However, it is still a probabilistic scheme, since the singlet state is extracted by the successive post-selections of transmitted events. The protocol presented here solves this problem, allowing one to produce a maximally entangled state of A and B from their arbitrary initial state *with probability 1*. The scheme remains free from the preparation and post-selection of the spin state of X .

The following is our protocol (see figure 3):

0. The initial state of A and B is *arbitrary* and is in general a mixed state ρ .
1. We send X with its spin *arbitrary* from the left to A and B with a resonant wave vector $k_n = n\pi/d$ ($n = 1, 2, \dots$), and see if it is transmitted to the right or reflected to the left, *irrespective of its spin state*.
2. If X is detected on the right (transmitted), we proceed to the next round (to step 1).
3. Otherwise (reflected), we send another X from the left with its spin *randomly* chosen with an off-resonant wave vector q (a perfectly polarized incident spin of X is not recommended). We do not check anything after this scattering; we just proceed to the next round (to step 1).
4. We repeat this routine (steps 1–3) many times and end with the singlet state $|\Psi^-\rangle_{AB}$ [TJ/F5711.955Tf5]

It is also worth stressing that, at step 1, the choice of the incident spin of X is irrelevant and we can choose it arbitrarily. At step 3, on the other hand, we can choose it randomly, but if the incident spin of X is perfectly polarized always in the same direction at every cycle, the scheme does not work. To make the following analysis simpler and transparent, however, we take unpolarized spin for both steps, represented by the completely mixed state $\mathbb{1}_X/2$.

A single cycle (steps 1–3) changes the spin state ρ of A and B in the following way

$$\rho \longrightarrow \mathcal{M}\rho = (\mathcal{T}_{k_n} + \mathcal{S}_q \mathcal{R}_{k_n})\rho, \quad (3.1)$$

where

$$\mathcal{T}_k \rho = \text{Tr}_X \{ T_k (\mathbb{1}_X/2 \otimes \rho) T_k^\dagger \}, \quad (3.2a)$$

$$\mathcal{R}_k \rho = \text{Tr}_X \{ R_k (\mathbb{1}_X/2 \otimes \rho) R_k^\dagger \} \quad (3.2b)$$

and

$$\mathcal{S}_k = \mathcal{T}_k + \mathcal{R}_k. \quad (3.3)$$

On the basis of the unitarity (2.3), the map \mathcal{M} is trace preserving,

$$\text{Tr}_{AB} \{ \mathcal{M}\rho \} = 1, \quad (3.4)$$

meaning that all possible outcomes are properly kept at each step and there is no selection of specific detection events.

We will see that repetition of the above cycle leads A and B into the singlet state,

$$\mathcal{M}^N \rho \rightarrow |\Psi^-\rangle_{AB} \langle \Psi^-| \quad (N \rightarrow \infty), \quad (3.5)$$

irrespective of their initial state ρ , where N is the number of cycles of the protocol. In other words, we are going to prove that \mathcal{M} is ‘mixing’ [11] with its fixed point given by $|\Psi^-\rangle_{AB} \langle \Psi^-|$.

4. Proof

In order to verify claim (3.5), we invoke an important result on mixing channels, which states that a completely positive and trace-preserving (CPT) map \mathcal{M} is mixing if it has a unique fixed point that is a pure state, e.g. see [11]. We remind the reader that the fixed points of \mathcal{M} are defined as those input states ρ_* that are left invariant by the action of the channel, that is

$$\mathcal{M}\rho_* = \rho_*. \quad (4.1)$$

In our case, we can immediately check that $|\Psi^-\rangle_{AB} \langle \Psi^-|$ is a fixed point of \mathcal{M} ; indeed, as is clear from equations (2.10a) and (2.10b), $|\Psi^-\rangle_{AB} \langle \Psi^-|$ is preserved by \mathcal{T}_{k_n} , while \mathcal{R}_{k_n} yields nothing (reflection does not occur with $|\Psi^-\rangle_{AB} \langle \Psi^-|$). Thus, since $|\Psi^-\rangle_{AB} \langle \Psi^-|$ is a pure state, it follows that the only thing we need to verify in order to prove the mixing (3.5) is that there exists no other fixed point of the channel \mathcal{M} .

Assume then that there exists another fixed point ρ_* , that is different from $|\Psi^-\rangle_{AB} \langle \Psi^-|$. By definition, it must satisfy the identity

$$\mathcal{M}\rho_* = (\mathcal{T}_{k_n} + \mathcal{S}_q \mathcal{R}_{k_n})\rho_* = \rho_*. \quad (4.2)$$

This expression can be simplified by noticing that the following identity holds at resonances

$$\mathcal{P}_- \mathcal{T}_{k_n} = \mathcal{P}_-, \quad (4.3)$$

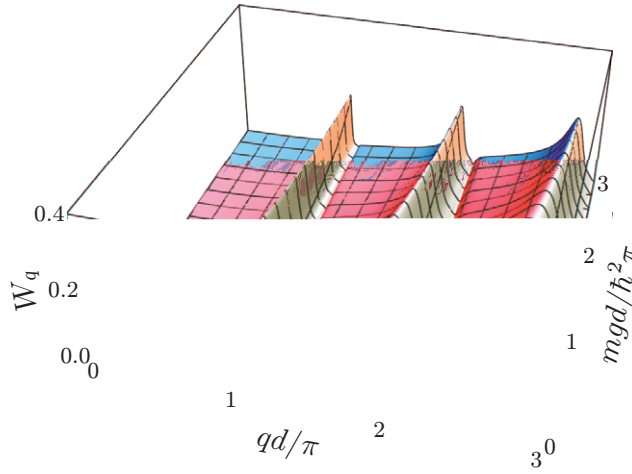


Figure 4. Coefficient W_q defined in equation (4.8) as a function of q and g . The larger the W_q , the larger the flow from the triplet sector to the singlet by the action of \mathcal{S}_q .

where \mathcal{P}_\pm are the superoperators associated with projections onto the triplet and singlet subspaces, respectively,

$$\mathcal{P}_\pm \rho = P_\pm \rho P_\pm. \quad (4.4)$$

Indeed, taking equation (4.3) into account, a necessary condition for equation (4.2) is given by

$$\mathcal{P}_- \mathcal{S}_q \mathcal{R}_{k_n} \rho_* = 0. \quad (4.5)$$

Looking at equation (2.10b) again, it shows that \mathcal{R}_{k_n} cuts out the singlet sector and acts on the triplet components. Since we are assuming that ρ_* is different from the singlet state $|\Psi^-\rangle_{AB} \langle \Psi^-|$, we must find some component $\mathcal{R}_{k_n} \rho_* \neq 0$ in the triplet sector. Therefore, if \mathcal{S}_q is a map that with certainty couples any triplet components to the singlet sector, condition (4.5) is never satisfied except for the singlet state $|\Psi^-\rangle_{AB} \langle \Psi^-|$. Consequently, the singlet state is proved to be the unique fixed point of the map \mathcal{M} .

The condition for such a map \mathcal{S}_q is expressed as

$$\text{Tr}_{AB} \{ \mathcal{P}_- \mathcal{S}_q \mathcal{P}_+ \rho \} > 0 \quad (4.6)$$

for any state $\rho \neq |\Psi^-\rangle_{AB} \langle \Psi^-|$. By inserting the explicit expressions of T_q and R_q given in equations (2.4a) and (2.4b), it reads

$$\text{Tr}_{AB} \{ \mathcal{P}_- \mathcal{S}_q \mathcal{P}_+ \rho \} = W_q \text{Tr}_{AB} \{ P_+ \rho \}, \quad (4.7)$$

with a coefficient

$$W_q = |\alpha_q|^2 \Omega_q^2 |1 - e^{2iqd}|^2 [4\Omega_q^2 + |1 - 2i\Omega_q + 3\Omega_q^2(1 - e^{2iqd})|^2], \quad (4.8)$$

which is nonvanishing for any $q \neq n\pi/d$ ($n = 0, 1, 2, \dots$) and for any state $\rho \neq |\Psi^-\rangle_{AB} \langle \Psi^-|$. That is, \mathcal{S}_q with an off-resonant wave vector q is a map that always couples any triplet component of A and B to the singlet sector and excludes the existence of ρ_* , satisfying equation (4.5) and differing from the singlet state $|\Psi^-\rangle_{AB} \langle \Psi^-|$. See figure 4, where coefficient W_q is plotted as a function of q and g . They are actually nonzero except at the resonant wave vectors $q = n\pi/d$ ($n = 1, 2, \dots$).

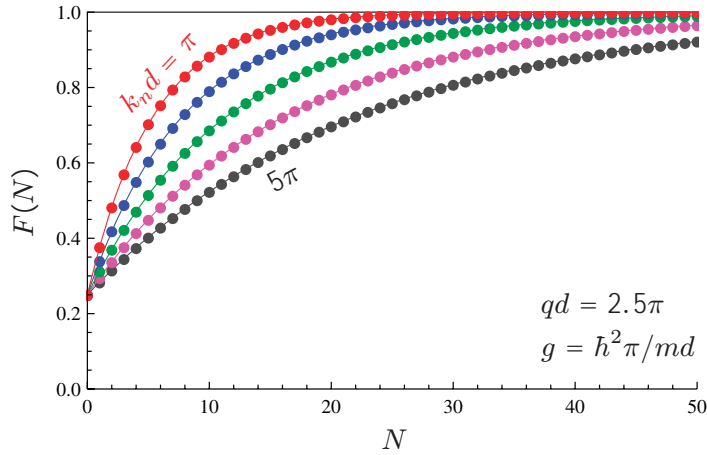


Figure 5. Average fidelity $F(N)$ defined in equation (4.9) as a function of the number N of protocol cycles. The five curves refer to different choices of the resonant wave vectors, namely $k_n d / \pi = 1, 2, 3, 4, 5$ from top to bottom. The other parameters are $q d / \pi = 2.5$ and $g = \hbar^2 \pi / m d$.

The reason A and B are attracted into the singlet state by repeated applications of \mathcal{M} is as follows. The singlet state $|\Psi^-\rangle_{AB} \langle\Psi^-|$ is the fixed point of the map \mathcal{M} , and the singlet component in the state of A and B remains there. As for the triplet components, they provoke the reflection of X with a certain probability at step 1. Once X is found to be reflected, qubits A and B are ‘shuffled’ by the subsequent off-resonant scattering \mathcal{S}_q , which creates a singlet component. In total, the probability of finding A and B in the singlet state is increased by the single cycle. Outflow of the probability from the singlet sector is absent, while inflow is present. This feature leads the system into the singlet state $|\Psi^-\rangle_{AB} \langle\Psi^-|$.⁷

The scheme works with certainty. As a direct check, the average fidelity $F(N)$ of the protocol is shown in figures 5 and 6. It is obtained by computing the fidelity between the generated state $\mathcal{M}^N \rho$ and the target $|\Psi^-\rangle_{AB} \langle\Psi^-|$, which is averaged over all possible choices of the input state ρ , that is

$$F(N) \equiv \overline{\text{Tr}_{AB}\{\mathcal{P}_- \mathcal{M}^N \rho\}} = \text{Tr}_{AB}\{\mathcal{P}_- \mathcal{M}^N (\mathbb{1}_{AB}/4)\}, \quad (4.9)$$

where $\overline{\dots}$ stands for the average over the input state ρ and $\mathbb{1}_{AB}$ is the identity operator on AB . From these plots, it is evident that as the number N of protocol cycles increases, the average fidelity $F(N)$ asymptotically approaches 1, as long as the wave vector q is properly set off-resonant. This implies that for an average choice of the input state ρ , the state $\mathcal{M}^N \rho$ approaches

⁷ One may wonder that a reflection event at step 1 suddenly projects out the singlet component and keeps A and B from approaching the singlet state. As the cycle is repeated, however, the average probability of finding A and B in the singlet state increases (as explained above), and the average probability of such a reflection occurring is accordingly reduced; the likelihood of the singlet component being lost is progressively lessened, and the singlet component keeps on growing on average. A simple statistical argument can then be used to claim that, since on average these events are suppressed, the probability of generating a specific trajectory that does not have this property is also suppressed.

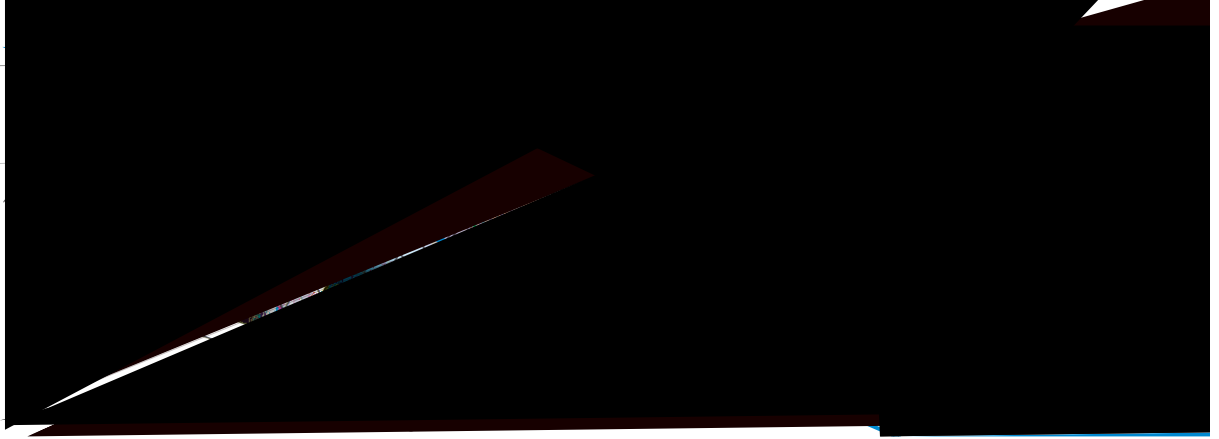


Figure 6. Average fidelity $F(N)$ defined in equation (4.9). (a) Dependence on q with $k_n = \pi/d$ and $g = \hbar^2\pi/md$. (b) Dependence on g with $k_n = \pi/d$ and $q = 2.5\pi/d$.

$|\Psi^-\rangle_{AB}\langle\Psi^-|$. By linearity, this also implies that the same result should hold for each input ρ .⁸ Therefore, figures 5 and 6 provide an alternative proof of the mixing property of \mathcal{M} .

The speed of the convergence is controlled by the following two factors: (i) the reflection of X sent with a resonant wave vector $k_n = n\pi/d$ ($n = 1, 2, \dots$), at step 1, due to the presence of triplet components in AB , and (ii) the transition of AB from the triplet sector to the singlet sector by off-resonant scattering with $q \neq n\pi/d$ ($n = 1, 2, \dots$), at step 3. Resonant scattering does not bring any triplet components of AB to the singlet sector at step 1. However, the reflection of the resonant X triggers us to proceed to the off-resonant scattering at step 3, which brings some triplet components of AB to the singlet sector. Therefore, the larger the reflection probability of the resonant X , and the stronger the transition from the triplet sector to the singlet by the off-resonant scattering, the faster the convergence to the fixed point. The former is controlled by R_{k_n} in equation (2.10b) and the latter by W_q in equation (4.8). In particular, the reflection probability is smaller for a higher incident wave vector k_n . See Ω_{k_n} in the numerator of R_{k_n} in equation (2.10b). W_q in equation (4.8) is also proportional to Ω_q^2 and is a decreasing function of q (for not too small q) (apart from the oscillation due to resonance). The convergence is thus slower with higher incident momenta, as demonstrated in figure 5.

5. Robustness

In this section, we analyze the robustness of the proposed scheme. We start by considering errors in the preparation of the ancilla qubits. Later, we analyze the effect of inefficient detectors.

5.1. Errors in the incident momentum

A key ingredient of our entanglement protocol is the resonant tunneling condition of the flying ancillas we impose at step 1. To see what happens if one fails to enforce such a constraint, we

⁸ As a matter of fact, one can easily verify that in the case of a pure fixed point, asymptotically optimal average fidelity is a sufficient condition for the mixing property of a CPT map.

consider two alternative scenarios. First, we analyze the case in which the source producing the ancilla qubits X is affected by a systematic error that forces it to produce a monochromatic sequence of particles that enters the 1D channel with a constant wave vector k , which is not resonant (error by deviation from resonance). Then, we consider the situation in which the same source is affected by fluctuations that prevent it from producing monochromatic signals (error by fluctuation of the incident momenta). For both scenarios, we compute the overlap between the final state of AB after N protocol cycles, and the target singlet state. As one might expect, the systematic error is much more detrimental to the performance of the protocol, with average fidelities that drop below 50% already for small deviations of the impinging momenta. On the other hand, the scheme appears to be more resilient to fluctuation errors.

5.1.1. Deviation from a resonance point. Assume that, at step 1 of the protocol, ancilla qubits X enter the 1D channel with fixed wave vector k , which is not necessarily at resonance. Following the derivation in section 3, one can easily verify that, after each protocol cycle, transformation of the state of AB can still be described as in equation (3.1), but with the superoperator \mathcal{M} replaced by the CPT map

$$\mathcal{M}_{k,q} = \mathcal{T}_k + \mathcal{S}_q \mathcal{R}_k. \quad (5.1)$$

Ideally, k should be set at resonance $k_n = n\pi/d$ ($n = 1, 2, \dots$), while q should be off-resonant. As shown in the previous section, these assumptions are sufficient to guarantee that the map $\mathcal{M} = \mathcal{M}_{k_n,q}$ is mixing with the singlet state as its fixed point. For $k \neq k_n$, however, this is not necessarily true, posing the problem of how to compute the state of AB in the asymptotic limit of large N (if $\mathcal{M}_{k,q}$ is not mixing, $\lim_{N \rightarrow \infty} \mathcal{M}_{k,q}^N \rho$ might not be well defined with the system continuously oscillating between different configurations [11]). For the sake of simplicity, however, we will neglect this issue in the following, assuming that the mixing property holds. Even though we do not have a formal proof for this property, such an assumption is strongly supported by a series of numerical calculations and the theoretical evidence. We remind the reader in fact that the mixing property of a CPT map is ultimately related to its spectrum [11]. Specifically, a necessary and sufficient condition for mixing is the existence of a finite gap between the largest and second largest eigenvalues of the map. As shown in figure 7, this seems to be the case for $\mathcal{M}_{k,q}$. Furthermore, since $\mathcal{M}_{k,q}$ depends continuously on k , its spectrum is a continuous function of k , and hence so is its mixing property. That is, there is at least a neighborhood of $k_n = n\pi/d$ ($n = 1, 2, \dots$) so that all $k \in (k_n - \varepsilon, k_n + \varepsilon)$ give rise to mixing maps. Finally, it is known that the set of nonmixing channels form a subset of zero measure in the set of CPT maps, so it is highly unlikely to have $\mathcal{M}_{k,q}$ nonmixing [10].

With the above considerations in mind, we identify the state of AB after $N \gg 1$ protocol cycles for generic k with the fixed point $\rho_*(k)$ of the map $\mathcal{M}_{k,q}$, that is

$$\mathcal{M}_{k,q} \rho_*(k) = \rho_*(k). \quad (5.2)$$

Interestingly enough, even without solving equation (5.2) explicitly, it is possible to derive a concise formula for its fidelity with respect to the singlet state,

$$F_*(k) \equiv \text{Tr}_{AB} \{ \mathcal{P}_- \rho_*(k) \}. \quad (5.3)$$

To see this, we first notice that the transitions between the singlet and triplet sectors of A and B induced by a single scattering event are described by the following 2×2 matrices: when X is

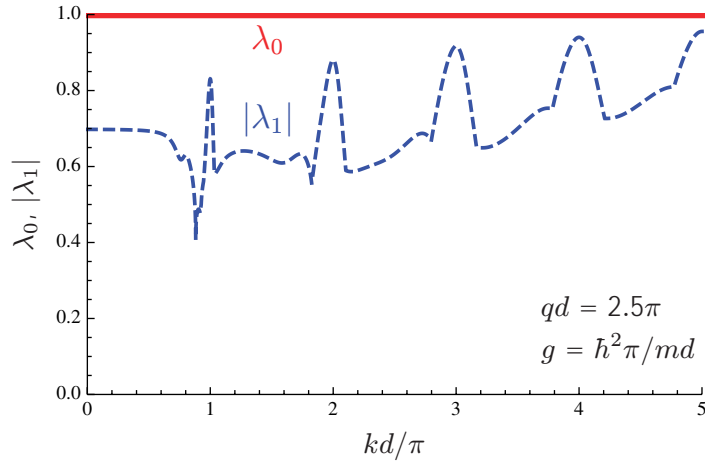


Figure 7. Magnitudes of the largest and second largest eigenvalues, λ_0 and λ_1 , of map $\mathcal{M}_{k,q}$ as a function of k with $q = 2.5\pi/d$ and $g = \hbar^2\pi/md$. The presence of a gap between them is a necessary and sufficient condition for mixing [11].

transmitted,

$$\begin{pmatrix} \text{Tr}_{AB}\{\mathcal{P}_-\mathcal{T}_k\rho\} \\ \text{Tr}_{AB}\{\mathcal{P}_+\mathcal{T}_k\rho\} \end{pmatrix} = \begin{pmatrix} \mathcal{T}_k^- & \mathcal{T}_k^{-+} \\ \mathcal{T}_k^{+-} & \mathcal{T}_k^{++} \end{pmatrix} \begin{pmatrix} \text{Tr}_{AB}\{\mathcal{P}_-\rho\} \\ \text{Tr}_{AB}\{\mathcal{P}_+\rho\} \end{pmatrix} \quad (5.4)$$

with

$$\mathcal{T}_k^{--} = |\alpha_k|^2 |1 - 4i\Omega_k - \Omega_k^2(1 - e^{2ikd})|^2, \quad (5.5a)$$

$$\mathcal{T}_k^{-+} = \frac{1}{3}\mathcal{T}_k^{+-} = 4|\alpha_k|^2 \Omega_k^4 |1 - e^{2ikd}|^2, \quad (5.5b)$$

$$\mathcal{T}_k^{++} = \frac{1}{9} |(\alpha_k + 2\beta_k) + 3\alpha_k \Omega_k^2(1 - e^{2ikd})|^2 + \frac{2}{9} |(\alpha_k - \beta_k) + 3\alpha_k \Omega_k^2(1 - e^{2ikd})|^2, \quad (5.5c)$$

and similarly, when X is reflected, with

$$\mathcal{R}_k^{--} = |1 - \alpha_k(1 - 4i\Omega_k) + \alpha_k \Omega_k^2(1 - e^{2ikd}) + 6i\alpha_k \Omega_k^3(1 - e^{2ikd})|^2, \quad (5.6a)$$

$$\mathcal{R}_k^{-+} = \frac{1}{3}\mathcal{R}_k^{+-} = |\alpha_k|^2 \Omega_k^2 |1 - e^{2ikd}|^2 |1 - 2i\Omega_k + 3\Omega_k^2(1 - e^{2ikd})|^2, \quad (5.6b)$$

$$\begin{aligned} \mathcal{R}_k^{++} = & \frac{1}{9} |3 - (\alpha_k + 2\beta_k) + i\Omega_k [2(\alpha_k - \beta_k) + 3i\alpha_k \Omega_k] (1 - e^{2ikd})|^2 \\ & + \frac{2}{9} |(\alpha_k - \beta_k) - i\Omega_k [(2\alpha_k + \beta_k) + 3i\alpha_k \Omega_k] (1 - e^{2ikd})|^2. \end{aligned} \quad (5.6c)$$

In this notation, W_q defined in equation (4.8) is expressed as $W_q = \mathcal{T}_q^{-+} + \mathcal{R}_q^{-+}$ and the 2×2 matrix for \mathcal{S}_q reads

$$\mathcal{S}_q = \begin{pmatrix} 1 - 3W_q & W_q \\ 3W_q & 1 - W_q \end{pmatrix}. \quad (5.7)$$

By abuse of notation, we use the same symbols for the corresponding 2×2 matrices, e.g. \mathcal{S}_q for the 2×2 matrix in equation (5.7). Combining these expressions, the matrix for $\mathcal{M}_{k,q}$ is also

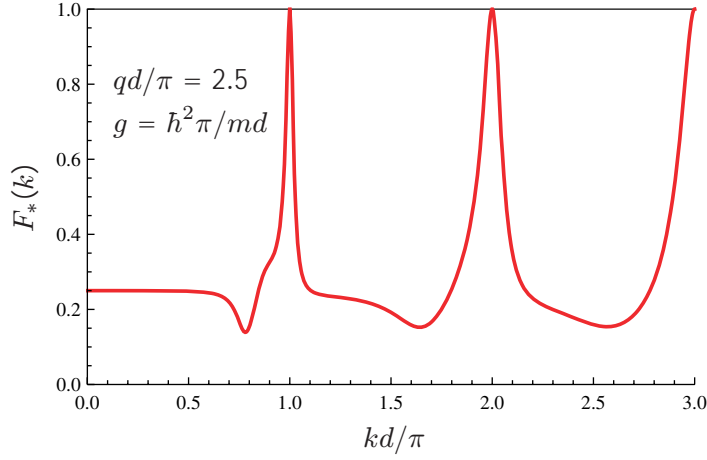


Figure 8. Fidelity $F_*(k)$ of the fixed point of the map $\mathcal{M}_{k,q}$ as a function of k for $q = 2.5\pi/d$ and $g = \hbar^2\pi/md$.

constructed according to equation (5.1). In particular, at resonances $k_n = n\pi/d$ ($n = 1, 2, \dots$), we have

$$\mathcal{T}_{k_n} = \begin{pmatrix} 1 & 0 \\ 0 & 1 - V_n \end{pmatrix}, \quad \mathcal{R}_{k_n} = \begin{pmatrix} 0 & 0 \\ 0 & V_n \end{pmatrix} \quad (5.8)$$

with

$$V_n = \frac{8\Omega_{k_n}^2 (1 + 8\Omega_{k_n}^2)}{(1 + 16\Omega_{k_n}^2)(1 + 4\Omega_{k_n}^2)}, \quad (5.9)$$

and for the ideal map,

$$\mathcal{M} = \mathcal{M}_{k_n,q} = \begin{pmatrix} 1 & W_q V_n \\ 0 & 1 - W_q V_n \end{pmatrix}. \quad (5.10)$$

Now, by noting equation (5.2), $\mathcal{P}_+ = 1 - \mathcal{P}_-$ and $\text{Tr}_{AB}\rho_*(k) = 1$, the definition of fidelity (5.3) is arranged as

$$\begin{aligned} F_*(k) &= \text{Tr}_{AB}\{\mathcal{P}_-\rho_*(k)\} \\ &= \text{Tr}_{AB}\{\mathcal{P}_-\mathcal{M}_{k,q}\rho_*(k)\} \\ &= \mathcal{M}_{k,q}^{--} \text{Tr}_{AB}\{\mathcal{P}_-\rho_*(k)\} + \mathcal{M}_{k,q}^{+-} \text{Tr}_{AB}\{\mathcal{P}_+\rho_*(k)\} \\ &= \mathcal{M}_{k,q}^{+-} + (\mathcal{M}_{k,q}^{--} - \mathcal{M}_{k,q}^{+-}) \text{Tr}_{AB}\{\mathcal{P}_-\rho_*(k)\} \\ &= \mathcal{M}_{k,q}^{+-} + (\mathcal{M}_{k,q}^{--} - \mathcal{M}_{k,q}^{+-}) F_*(k). \end{aligned} \quad (5.11)$$

Therefore, as long as $1 - \mathcal{M}_{k,q}^{--} + \mathcal{M}_{k,q}^{+-} > 0$ (which is assured by $\mathcal{M}_{k,q}^{+-} > 0$ or $\mathcal{M}_{k,q}^{--} < 1$), one obtains a concise formula for the fidelity

$$F_*(k) = \frac{\mathcal{M}_{k,q}^{+-}}{1 - \mathcal{M}_{k,q}^{--} + \mathcal{M}_{k,q}^{+-}}. \quad (5.12)$$

In figure 8, we report its plot as a function of the incident wave vector k for a fixed q ; as anticipated, the fidelity $F_*(k)$ drops below 50% as k deviates from a resonance point $k_n = n\pi/d$ ($n = 1, 2, \dots$) by less than a per cent.

5.1.2. Wave packet or fluctuation of the incident momenta. Consider now the case in which the source emitting X injects a stream of non-monochromatic ancillas into the 1D channel. Specifically, let $\psi(k)$ and $\phi(q)$ represent the wave packets in momentum space of the particles produced by the source at steps 1 and 3 of the protocol, respectively. Then, the map $\mathcal{M}_{k,q}$ of the previous section is substituted by⁹

$$\tilde{\mathcal{M}} = \int_0^\infty dk \int_0^\infty dq |\psi(k)|^2 |\phi(q)|^2 \mathcal{M}_{k,q}. \quad (5.13)$$

Note that the trace over the momentum degrees of freedom is taken since the detectors do not resolve the momenta, and as a result only diagonal components with respect to the momenta contribute to the formula. This implies that a different type of fluctuation in momentum, incoherent fluctuation, is described by what is formally the same formula as equation (5.13). Indeed, suppose that the incident wave vectors k and q differ from run to run. Then, the state generated after N cycles of the protocol reads

$$\rho_{(k_1, q_1), \dots, (k_N, q_N)} = \mathcal{M}_{k_N, q_N} \cdots \mathcal{M}_{k_1, q_1} \rho. \quad (5.14)$$

If the fluctuations of the momenta (k_i, q_i) at each cycle $i = 1, \dots, N$ are characterized by a common probability distribution function $f(k_i, q_i)$, state (5.14) averaged over the probability distribution reads

$$\tilde{\rho}(N) = \int \left(\prod_{i=1}^N dk_i dq_i f(k_i, q_i) \right) \rho_{(k_1, q_1), \dots, (k_N, q_N)} = \tilde{\mathcal{M}}^N \rho, \quad (5.15)$$

where in this case

$$\tilde{\mathcal{M}} = \int_0^\infty dk \int_0^\infty dq f(k, q) \mathcal{M}_{k,q}, \quad (5.16)$$

which coincides with the expression of equation (5.13) by identifying $f(k, q)$ with $|\psi(k)|^2 |\phi(q)|^2$.

It is worth stressing that, in contrast to the case treated in the previous subsection, one can show that the average map $\tilde{\mathcal{M}}$ is mixing, provided that the distribution $f(k, q)$ overlaps with a resonant wave vector in k and has only measure zero in q at resonances. Indeed, we can split $\tilde{\mathcal{M}}$ into two parts as

$$\tilde{\mathcal{M}} = \int_{k_n - \varepsilon}^{k_n + \varepsilon} dk \int_0^\infty dq f(k, q) \mathcal{M}_{k,q} + \tilde{\mathcal{M}}'. \quad (5.17)$$

Recall then that any nontrivial convex sum of a mixing map \mathcal{E} and something else \mathcal{E}' (not necessarily mixing),

$$\tilde{\mathcal{E}} = \lambda \mathcal{E} + (1 - \lambda) \mathcal{E}' \quad (0 < \lambda \leq 1), \quad (5.18)$$

is also a mixing map [10]. Since the first part of equation (5.17) is mixing, and has measure nonzero, this theorem ensures that $\tilde{\mathcal{M}}$ is also mixing, implying that the mixing property of $\tilde{\mathcal{M}}$ is robust against the momentum fluctuation. As a consequence, in the limit of infinitely many protocol cycles, system AB is driven to the fixed point $\tilde{\rho}_*$ of channel $\tilde{\mathcal{M}}$ in equation (5.16).

⁹ We assume that the wave packets are composed of only positive momenta. It is possible to show, however, that the presence of negative momenta does not spoil the mixing property to be argued for in this section. In any case, it seems reasonable to assume that such components are negligibly small.

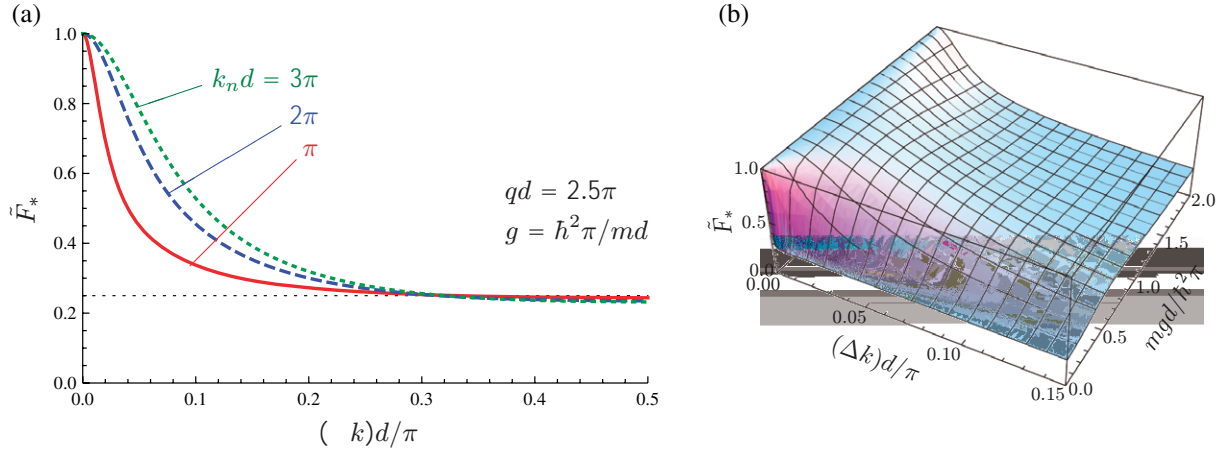


Figure 9. Average fidelity \tilde{F}_* given in equation (5.19) of the fixed point of map $\tilde{\mathcal{M}}$ for a Gaussian distribution of k in equation (5.20): (a) as a function of Δk for different resonant wave vectors $k_n d/\pi = 1$ (solid), 2 (dashed), 3 (dotted), with $qd/\pi = 2.5$ and $g = \hbar^2\pi/md$ and (b) as a function of Δk and g with $k_n d/\pi = 1$ and $qd/\pi = 2.5$.

Its fidelity with respect to the singlet state can now be computed similarly to equation (5.12), yielding

$$\tilde{F}_* \equiv \text{Tr}_{AB}\{\mathcal{P}_-\tilde{\rho}_*\} = \frac{\tilde{\mathcal{M}}^{+-}}{1 - \tilde{\mathcal{M}}^{--} + \tilde{\mathcal{M}}^{+-}}, \quad (5.19)$$

where matrix elements $\tilde{\mathcal{M}}^{\pm\pm}$ are obtained by averaging $\mathcal{M}_{k,q}^{\pm\pm}$ over the distribution $f(k, q)$.

In figure 9, the fidelity \tilde{F}_* is plotted for a Gaussian distribution of k , centered at a resonance k_n with width Δk , for a fixed q ,

$$f(k, q) \propto \theta(k) e^{-(k-k_n)^2/2(\Delta k)^2} \delta(q - \bar{q}), \quad (5.20)$$

which is normalized as $\int_0^\infty dk \int_0^\infty dq f(k, q) = 1$. As expected, the fidelity \tilde{F}_* decreases from unity, as the width of the distribution Δk grows. Notably, in this case the scheme seems to be quite resilient to the noise; the fidelity drops below 50% only for $\Delta k/k_n$ of the order of 5%. Furthermore, the decrease is slower than linear for sufficiently small Δk , and is less pronounced for larger central resonant wave vector k_n and a smaller (but not too small) coupling constant g (although the approach to the final state is slower with a larger k_n , as demonstrated in figure 10).

5.2. Detector efficiency

In this section, we analyze how defective detections of scattered ancillas diminish the protocol's performance. In particular, we consider the case in which the detectors in figure 1 are characterized by an efficiency $\eta < 1$, i.e. they fail to report the arrival of a particle X with probability $1 - \eta$ (for the sake of simplicity, we assume that the two detectors have the same efficiency η).

To account for such events, we need to specify the action required when the detectors fail to report the arrival of a scattered particle incident on resonance at step 1 of the protocol (since

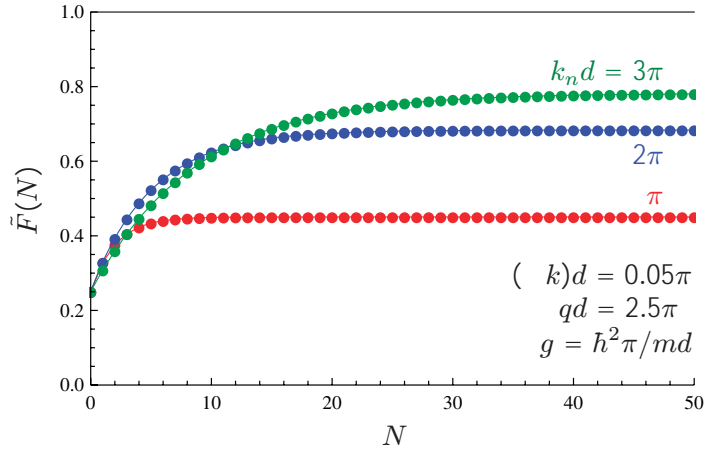


Figure 10. Average fidelity $\tilde{F}(N) = \text{Tr}_{AB}\{\mathcal{P}_-\tilde{\mathcal{M}}^N(\mathbb{1}_{AB}/4)\}$ as a function of number N of protocol cycles, for a Gaussian distribution of k in equation (5.20). The three curves refer to different choices of the resonant wave vectors, namely $k_n d/\pi = 1, 2, 3$, with the other parameters fixed at $(\Delta k)d/\pi = 0.05$, $qd/\pi = 2.5$, and $g = \hbar^2\pi/md$.

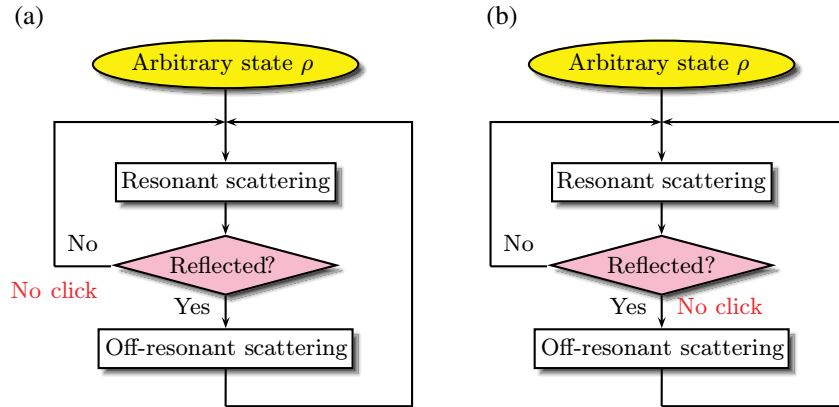


Figure 11. Flowcharts for cases I (a) and II (b).

we do not check anything after the scattering of an off-resonant particle at step 3, the efficiency of the detector does not matter for this step). Specifically, we analyze two alternative solutions.

Case I: we may simply proceed to the next round (step 1) and send the next particle on resonance (figure 11(a)). In such a case, map \mathcal{M} is modified to

$$\mathcal{M}_\eta^{(1)} = \eta\mathcal{M} + (1 - \eta)\mathcal{S}_{k_n}, \quad (5.21)$$

which is still mixing by the same argument for equation (5.17). By noting the expressions in equations (5.7) and (5.10), its 2×2 matrix that describes the transitions between singlet and triplet sectors reads

$$\mathcal{M}_\eta^{(1)} = \begin{pmatrix} 1 & \eta W_q V_n \\ 0 & 1 - \eta W_q V_n \end{pmatrix}, \quad (5.22)$$

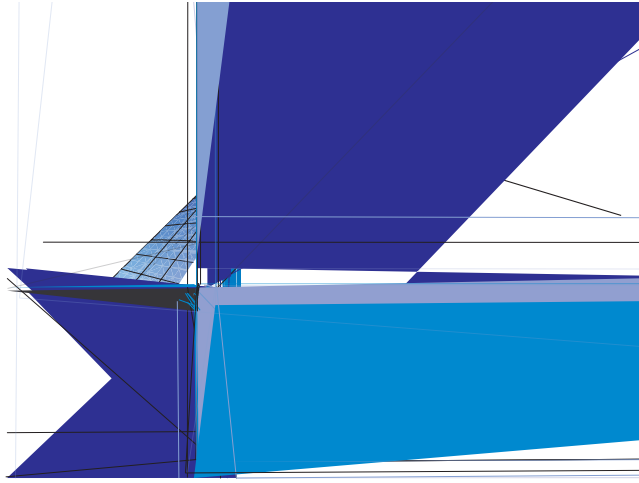


Figure 12. Plot of the average fidelity $F^{(1)}(N) = \text{Tr}_{AB}\{\mathcal{P}_-\mathcal{M}_\eta^{(1)N}(\mathbb{1}_{AB}/4)\}$ for inefficient detectors, with the strategy described in case I of section 5.2. N is the number of protocol cycles and η is detector efficiency. The other parameters are $k_n = \pi/d$, $q = 2.5\pi/d$ and $g = \hbar^2\pi/md$.

and by applying the formula (5.12), the fidelity of its fixed point to the target singlet state is shown to remain

$$F_*^{(1)}(\eta) = 1. \quad (5.23)$$

The protocol is therefore still able to extract the singlet state from AB . Notice, however, that the speed of the convergence of the scheme is affected by $\eta < 1$, as shown in figure 12. This is a consequence of the fact that, in this case, the element of the scattering matrix (5.22) associated with the transition from the triplet sector to the singlet sector gets degraded; the smaller the η , the slower the speed of convergence.

Case II: We can proceed to step 3 (as if the ancilla X on resonance is reflected) and send X with the off-resonant wave vector q (figure 11(b)). In this case, map \mathcal{M} is changed to

$$\mathcal{M}_\eta^{(2)} = \eta\mathcal{M} + (1 - \eta)\mathcal{S}_q\mathcal{S}_{k_n}, \quad (5.24)$$

which is also mixing. It yields

$$\mathcal{M}_\eta^{(2)} = \begin{pmatrix} 1 - 3(1 - \eta)W_q & (1 - \eta + \eta V_n)W_q \\ 3(1 - \eta)W_q & 1 - (1 - \eta + \eta V_n)W_q \end{pmatrix}, \quad (5.25)$$

and the fidelity of its fixed point is given by

$$F_*^{(2)}(\eta) = \frac{(1 - \eta) + \eta V_n}{4(1 - \eta) + \eta V_n}, \quad (5.26)$$

which ranges between 0.25 and 1. This strategy is thus not as effective as the previous one in terms of fidelity. This is because the off-resonant scattering in the absence of a guarantee that there is no singlet component in AB , which should be ensured by the detection of a reflected

particle on resonance, provokes the undesired transition from the singlet sector to the triplet sector. The presence of this leakage channel hinders convergence to the singlet state.

6. Conclusions and remarks

We have proposed and studied a scheme for preparing a maximally entangled state in two noninteracting qubits, initially given in an arbitrary state. By repetition of resonant scattering of ancilla qubit, followed by off-resonant scattering if necessary, qubits A and B are driven from any initial state into the singlet state with probability 1 (perfect efficiency). Neither the preparation nor the post-selection of the ancilla spin state is required. By introducing an appropriate feedback strategy, the previously proposed probabilistic scheme has been turned into a reiterative scheme, which leads the target qubits to the singlet state with a probability that converges asymptotically to 1 in the number of iterations. It is remarkable that no additional element or technology is required for the feedback; we have only to set the incident momentum of the ancilla off a resonance point. The convergence to the unique fixed point (mixing property) is rigorously proved, and is shown to be robust against various types of imperfection in the scheme. In particular, the scheme is very robust against the inefficiency of the detectors, which is clarified by a concise formula for the fidelity of the fixed point of the mixing map to the target singlet state.

We have here concentrated on a specific physical model with two qubits fixed along a 1D channel, where ancilla qubits flow. The present analysis, however, provides a general guideline for turning a probabilistic convergence scheme into a scheme that works with probability arbitrarily close to 1. In general, the former probabilistic scheme keeps the target state, as long as the measurement on an ancilla reports the desired result. If the measurement outcome is not the desired one and if in such a case we are sure that the system is in an orthogonal state to the target, it is quite easy to design the feedback; we simply ‘shake’ the system to provoke the transition from the orthogonal state to the target state. This inflow to the target state, in the absence of outflow, ensures convergence to the target state. Note also that the methods given in [10] can be interpreted as feedback schemes for [2]. The methods developed for these simple systems pave the way for general strategies for driving systems to target states.

Acknowledgments

This work was supported by a Special Coordination Fund for Promoting Science and Technology and a Grant-in-Aid for Young Scientists (B) (no. 21740294), both from the Ministry of Education, Culture, Sports, Science and Technology, Japan; by a Grant-in-Aid for Scientific Research (C) from the Japan Society for the Promotion of Science; by the Italian Ministry of University and Research under the bilateral Italian–Japanese Projects II04C1AF4E on ‘Quantum Information, Computation and Communication’ and the FIRB IDEAS project ESQUI; by the Joint Italian–Japanese Laboratory on ‘Quantum Information and Computation’ of the Italian Ministry for Foreign Affairs; and by the EPSRC grant EP/F043678/1.

References

- [1] Nielsen M A and Chuang I L 2000 *Quantum Computation and Quantum Information* (Cambridge: Cambridge University Press)
- Bouwmeester D, Zeilinger A and Ekert A 2000 *The Physics of Quantum Information: Quantum Cryptography, Quantum Teleportation, Quantum Computation* (Berlin: Springer)
- Bennett C H and DiVincenzo D P 2000 *Nature* **404** 247
- Galindo A and Martín-Delgado M A 2002 *Rev. Mod. Phys.* **74** 347
- [2] Nakazato H, Takazawa T and Yuasa K 2003 *Phys. Rev. Lett.* **90** 060401
- [3] Nakazato H, Unoki M and Yuasa K 2004 *Phys. Rev. A* **70** 012303
- [4] Wu L A, Lidar D A and Schneider S 2004 *Phys. Rev. A* **70** 032322
- Paternostro M and Kim M S 2005 *New J. Phys.* **7** 43
- [5] Militello B and Messina A 2004 *Phys. Rev. A* **70** 033408
- [6] Compagno G, Messina A, Nakazato H, Napoli A, Unoki M and Yuasa K 2004 *Phys. Rev. A* **70** 052316
- Yuasa K and Nakazato H 2005 *Prog. Theor. Phys.* **114** 523
- [7] Ciccarello F, Paternostro M, Kim M S and Palma G M 2008 *Phys. Rev. Lett.* **100** 150501
- Ciccarello F, Paternostro M, Palma G M and Zarcone M 2008 *Int. J. Quant. Info.* **6** 759
- [8] Yuasa K 2009 arXiv:0908.4377
- [9] Ciccarello F, Paternostro M, Palma G M and Zarcone M 2009 *New J. Phys.* **11** 113053
- [10] Giovannetti V and Burgarth D 2006 *Phys. Rev. Lett.* **96** 030501
- Burgarth D and Giovannetti V 2007 *Phys. Rev. A* **76** 062307
- Burgarth D and Giovannetti V 2008 *Quantum Information and Many Body Quantum Systems: Proc. ed M Ericsson and S Montangero* (Pisa: Edizioni della Normale) p 17
- [11] Burgarth D and Giovannetti V 2007 *New J. Phys.* **9** 150
- [12] Bruneau L, Joye A and Merkli M 2006 *J. Funct. Anal.* **239** 310
- [13] Costa Jr A T, Bose S and Omar Y 2006 *Phys. Rev. Lett.* **96** 230501
- Giorgi G L and de Pasquale F 2006 *Phys. Rev. B* **74** 153308
- Yuasa K and Nakazato H 2007 *J. Phys. A: Math. Theor.* **40** 297
- Ciccarello F, Palma G M, Zarcone M, Omar Y and Vieira V R 2007 *J. Phys. A: Math. Theor.* **40** 7993
- Ciccarello F, Palma G M, Zarcone M, Omar Y and Vieira V R 2007 *Laser Phys.* **17** 889
- Habgood M, Jefferson J H and Briggs G A D 2008 *Phys. Rev. B* **77** 195308
- Habgood M, Jefferson J H and Briggs G A D 2009 *J. Phys.: Condens. Matter* **21** 075503
- [14] Ciccarello F, Palma G M, Zarcone M, Omar Y and Vieira V R 2006 *New J. Phys.* **8** 214
- [15] Hida Y, Nakazato H, Yuasa K and Omar Y 2009 *Phys. Rev. A* **80** 012310
- [16] Datta S 1997 *Electronic Transport in Mesoscopic Systems* (Cambridge: Cambridge University Press)
- [17] Tans S J, Devoret M H, Dai H, Thess A, Smalley R E, Geerligs L J and Dekker C 1997 *Nature* **386** 474